

Proceedings of the Second Annual LHCP

September 16, 2014

Measurements of hadron production in p -Pb collisions at LHCf

GAKU MITSUKA

*On behalf of the LHCf Collaboration,
University of Florence and INFN Firenze,
Via Sansone 1, 50019 Sesto Fiorentino (Fi), Italy*

ABSTRACT

The transverse momentum distribution for inclusive neutral pions in very forward rapidity region has been measured with the LHCf detector in p -Pb collisions at nucleon-nucleon center-of-mass energies of $\sqrt{s_{NN}} = 5.02$ TeV at the LHC. The transverse momentum spectra obtained in p -Pb collisions show a strong suppression of the production of neutral pions relative to the spectra in p - p collisions at $\sqrt{s} = 5.02$ TeV. The nuclear modification factor is about 0.1–0.4, which overall agrees with the predictions of several hadronic interaction Monte Carlo simulations. Furthermore the recent results on the inclusive energy spectra of forward neutrons in p - p collisions at $\sqrt{s} = 7$ TeV will be discussed.

PRESENTED AT

The Second Annual Conference
on Large Hadron Collider Physics
Columbia University, New York, U.S.A
June 2-7, 2014

1 Introduction

The Large Hadron Collider forward (LHCf) experiment [1] has been designed to measure the hadronic production cross sections of neutral particles emitted in very forward angles, including zero degrees, in proton-proton (p - p) and proton-lead (p -Pb) collisions at the LHC. The LHCf detectors have the capability for precise measurements of forward high-energy inclusive-particle-production cross sections of photons, neutrons, and other neutral mesons and baryons. The discussions in this proceeding concentrate on (1) the inclusive production rate for neutral pions (π^0 's) in the rapidity range $-11.0 < y_{\text{lab}} < -8.9$ as a function of the π^0 transverse momentum, and (2) the inclusive production rate for neutrons in the pseudo-rapidity range $\eta > 8.81$ as a function of the neutron energy.

This work is motivated by an application to the understanding of ultrahigh-energy cosmic ray (UHECR) phenomena, which are sensitive to the particle productions driven by soft and semi-hard QCD at extremely high energy. Although UHECR observations have made notable advances in the last few years, critical parts of the analysis depend on Monte Carlo (MC) simulations of air shower development that are sensitive to the choice of the hadronic interaction model. The fact that the lack of knowledge about forward particle production in hadronic collisions hinders the interpretation of observations of UHECR was studied in other documents, for example see Ref. [2].

This proceedings is organized as follows. In Sec. 2 the LHCf detectors are described. The analyses results are then presented in Sec. 3 and Sec. 4.

2 The LHCf detectors

Two independent LHCf detectors, called Arm1 and Arm2, have been installed in the instrumentation slots of the target neutral absorbers (TANs) [3] located ± 140 m from the ATLAS interaction point (IP1) and at zero degree collision angle. Charged particles produced at IP1 and directed towards the TAN are swept aside by the inner beam separation dipole magnet D1 before reaching the TAN. Therefore only neutral particles produced at IP1 enter the LHCf detector. At this location the LHCf detectors cover the pseudo-rapidity range from 8.7 to infinity for zero degree beam crossing angle. With a maximum beam crossing angle of $140 \mu\text{rad}$, the pseudo-rapidity range can be extended to 8.4 to infinity. The structure and performance of the LHCf detectors are explained in Ref. [4].

3 Transverse momentum spectra of neutral pions in p -Pb collisions at $\sqrt{s_{NN}} = 5.02 \text{ TeV}$

Data used in the analysis in this section were taken in three different runs; The first run was taken in LHC Fill 3478 and the second and third runs were taken in LHC Fill 3481. The integrated luminosity of the data was 0.63 nb^{-1} after correcting for the live time of data acquisition systems.

The p_T spectrum in the rapidity range $-9.4 < y_{\text{lab}} < -9.2$ is presented in Fig. 1. The spectra categorized into other five ranges of rapidity, $[-9.0, -8.9]$, $[-9.2, -9.0]$, $[-9.6, -9.4]$, $[-10.0, -9.6]$, and $[-11.0, -10.0]$, are found in Ref. [5]. The inclusive π^0 production rate is defined as

$$\frac{1}{\sigma_{\text{inel}}^{\text{pPb}}} E \frac{d^3 \sigma^{\text{pPb}}}{dp^3} = \frac{1}{N_{\text{inel}}^{\text{pPb}}} \frac{d^2 N^{\text{pPb}}(p_T, y)}{2\pi p_T dp_T dy}. \quad (1)$$

where $\sigma_{\text{inel}}^{\text{pPb}}$ is the inelastic cross section for p -Pb collisions at $\sqrt{s_{NN}} = 5.02 \text{ TeV}$ and $E d^3 \sigma^{\text{pPb}}/dp^3$ is the inclusive cross section of π^0 production. The number of inelastic collisions $N_{\text{inel}}^{\text{pPb}}$ in this analysis is 9.33×10^7 . $d^2 N^{\text{pPb}}(p_T, y)$ is the number of π^0 's detected in the transverse momentum interval (dp_T) and the rapidity interval (dy) with all corrections applied.

In the left panel of Fig. 1, the filled circles represent the data from the LHCf experiment. The error bars and shaded rectangles indicate the one-standard-deviation statistical and total systematic uncertainties respectively. The total systematic uncertainties are given by adding all uncertainty terms except the one

for luminosity in quadrature. When the impact parameter of beam proton and beam Pb is larger than the overlapping radii of each particle, so-called ultra-peripheral collisions (UPCs) can occur. The contribution from UPCs is presented as open squares in the left panel of Fig. 1 (normalized to 1/2 for visibility). The estimation of the energy and momentum spectra of the UPC-induced π^0 's is discussed in Ref. [5] and the comparison with the prediction of a hadronic interaction model which contains no UPC contribution is shown in the right panel of Fig. 1.

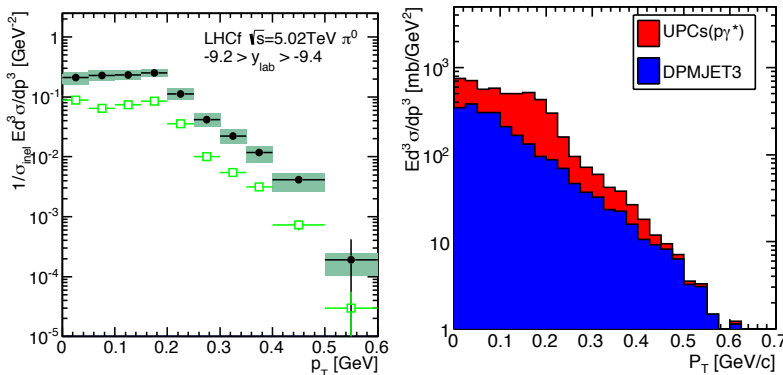


Figure 1: (Left) Filled circles indicate experimental p_T spectra of the LHCf detector. The open squares indicate the estimated contribution from UPCs. (Right) Estimated p_T spectra of UPC-induced π^0 's (red shaded area) and the prediction of a typical hadronic interaction model (DPMJET 3.04, blue shaded area).

Figure 2 shows the LHCf data p_T spectra after subtraction of the UPC component (filled circles). The error bars correspond to the size of total uncertainties including both statistical and systematic uncertainties. The p_T spectra in p -Pb collisions at 5.02 TeV predicted by the hadronic interaction models, DPMJET 3.04 [6] (solid line, red), QGSJET II-03 [7] (dashed line, blue), and EPOS 1.99 [8] (dotted line, magenta), are also shown in the same figure for comparison. Predictions by the three hadronic interaction models do not include the UPC component. Among the predictions given by the hadronic interaction models tested here, DPMJET 3.04 and EPOS 1.99 show a good overall agreement with the LHCf measurements.

Finally the nuclear modification factor R_{pPb} is derived in Fig. 3. The nuclear modification factor is defined as

$$R_{pPb} \equiv \frac{\sigma_{inel}^{pp}}{\langle N_{coll} \rangle \sigma_{inel}^{pPb}} \frac{Ed^3\sigma^{pPb}/dp^3}{Ed^3\sigma^{pp}/dp^3}, \quad (2)$$

where $Ed^3\sigma^{pPb}/dp^3$ and $Ed^3\sigma^{pp}/dp^3$ are the inclusive cross sections of π^0 production in p -Pb and p - p collisions at 5.02 TeV respectively. The average number of binary nucleon-nucleon collisions in a p -Pb collision is $\langle N_{coll} \rangle = 6.9$.

The LHCf measurements, currently having a large uncertainty which increases with p_T mainly due to systematic uncertainties in p -Pb collisions at 5.02 TeV, show a strong suppression with R_{pPb} from 0.1 to 0.4 depending on p_T . All hadronic interaction models predict small values of $R_{pPb} \approx 0.1$, and they show an overall good agreement with the LHCf measurements within the uncertainty.

4 Energy spectra of neutrons in p - p collisions at $\sqrt{s} = 7$ TeV

In this section we show the energy spectra of neutrons in p - p collisions at $\sqrt{s} = 7$ TeV. The measured energy spectra obtained from the two independent calorimeters of Arm1 and Arm2 in the pseudo-rapidity η ranging from 8.81 to 8.99, from 8.99 to 9.22, and from 10.76 to infinity, are shown in Fig. 4. The similar characteristic features are found between the Arm1 and Arm2 measurements in all ranges even before unfolding the spectra. The slight, but apparent, differences between the two detectors can be understood by the detector response in each detector.

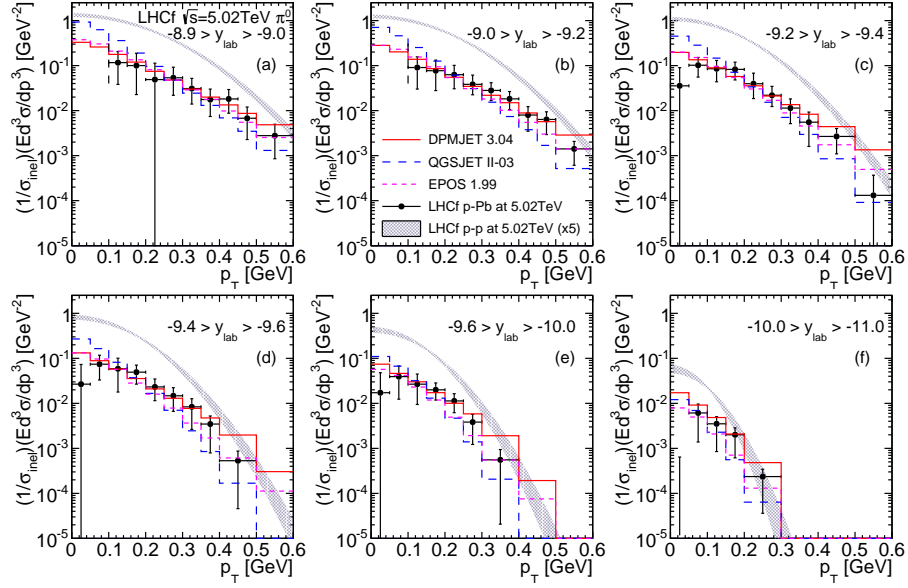


Figure 2: Filled circles indicate experimental p_T spectra measured by LHCf after the subtraction of the UPC component. Hadronic interaction models predictions and derived spectra for p - p collisions at 5.02 TeV are also shown.

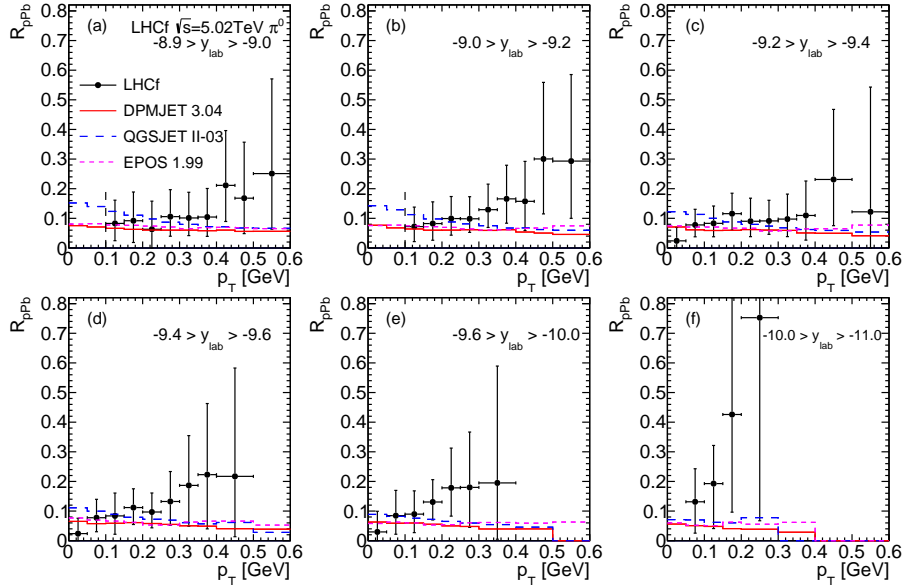


Figure 3: Filled circles indicate the nuclear modification factors obtained by the LHCf measurements. Other lines are the predictions by hadronic interaction models hadronic interaction models: DPMJET 3.04 (red solid line), QGSJET II-03 (blue dashed line), and EPOS 1.99 (magenta dotted line).

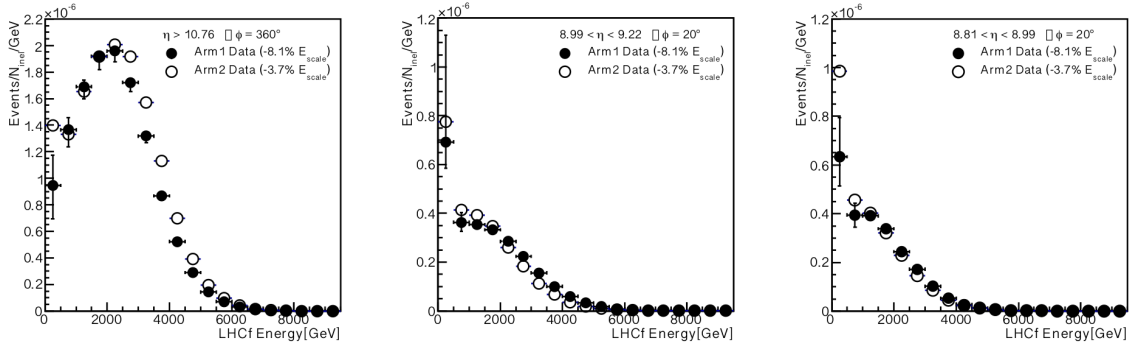


Figure 4: Energy spectra of neutrons measured by the Arm1 (filled circles) and the Arm2 detectors (open circles).

Figure 5 shows the combined Arm1 and Arm2 spectra with all corrections and spectra unfolding applied. The experimental results indicate that the highest neutron production rate occurs at the most forward rapidity range ($\eta > 10.76$) compared with the hadronic interaction models. QGSJET II-03 predicts a neutron production rate compatible with the experimental results at the most forward rapidity. On the other hand, DPMJET 3.04 shows the best agreement with the experimental results at other two rapidity ranges.

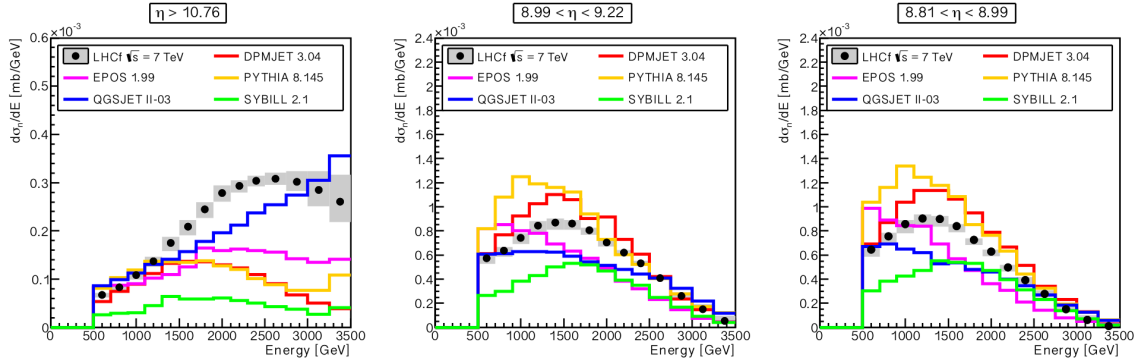


Figure 5: Energy spectra of neutrons obtained by combining with the Arm1 and Arm2 measurements (filled circles and shaded areas show the combined results and the systematic errors, respectively). Other colored lines are the predictions by hadronic interaction models.

References

- [1] LHCf Technical Design Report, CERN-LHCC-2006-004
- [2] R. Ulrich, R. Engel and M. Unger, Phys. Rev. D **83**, 054026 (2011).
- [3] W. C. Turner, E. H. Hoyer and N. V. Mokhov, Proc. of EPAC98, Stockholm, 368 (1998). LBNL Rept. LBNL-41964 (1998).
- [4] O. Adriani, *et al.*, Int. J. Mod. Phys. A, **28**, 1330036 (2013).
- [5] O. Adriani, *et al.*, Phys. Rev. **C89**, 065209 (2014).
- [6] F. W. Bopp, J. Ranft, R. Engel and S. Roesler, Phys. Rev. **C77**, 014904 (2008).

- [7] S. Ostapchenko, Nucl. Phys. Proc. Suppl. **151**, 143 (2006).
- [8] K. Werner, F.-M. Liu and T. Pierog, Phys. Rev. **C74**, 044902 (2006).